



Gazi University

Journal of Science

PART A: ENGINEERING AND INNOVATION

<http://dergipark.org.tr/guj.1466745>

Evaluating the Spatial-Temporal Dynamics of Urbanization in Prefecture Cities of China Using SNPP-VIIRS Nighttime Light Remote Sensing Data

Neel Chaminda WITHANAGE^{1,2*} Jingwei SHEN² ¹ University of Ruhuna, Faculty of Humanities and Social Sciences, Department of Geography, Matara 81000, Sri Lanka² Southwest University, School of Geographical Sciences, Bebei District 400715, Chongqing Province, China

Keywords	Abstract
China	Ensuring the well-being of urban communities hinges on sustainable urban planning strategies informed by current data, particularly in China since urbanization has been one of the most significant demographic shifts in recent decades. Therefore, our research aimed to evaluate the spatio-temporal dynamics of urbanization and sub urbanization across prefecture and provincial levels in China by utilizing consistent SNPP-VIIRS-like and NPP-VIIRS nighttime data spanning the years 2000 to 2020. The k-means method was applied to derive urban and sub urban features from above datasets. The findings uncovered a significant expansion of urban entities at the prefecture level, escalating from 16,209 km ² to 89,631 km ² over the specified period showing a 5% growth. Among five main urban agglomerations, the Yangtze River Delta stands out with the highest urbanization rate, witnessing a remarkable expansion of urban entities from 2,684 km ² to 41,465 km ² . This growth reflects an average growth rate of 72.2% per annum. The analysis revealed that the overall area of suburbs expanded from 59,151 km ² to 120,339 km ² between 2012 and 2020 indicating a proportional growth rate ranging from 0.4% to 1.9%. The peak growth rate of suburbs was recorded between 2012 and 2014, reaching 18%. Guizhou, Hunan, and Hubei provinces have exhibited growth rates of 334%, 258%, and 246% respectively while Beijing, Guangdong, Tianjin, and Shanghai have experienced relatively low growth rates of 50%, 56%, 46%, and 17%. The analysis of urban growth with GDP, population, and electricity consumption revealed an inverse relationship during the specified period. Therefore, the findings of this research can provide immense support to sustainable urban planning initiatives at both the provincial and prefecture-level cities in China. The findings can assist city planning authorities in making informed decisions regarding optimizing resource distribution, all while prioritizing the preservation of ecological footprint within urban environments. Also, the limitations addressed in our study must be taken into account in future research works aimed at deriving reliable urban extraction results using nighttime light remote sensing data.
Nighttime Light	
Prefectures Cities	
Remote Sensing	
SNPP-VIIRS	
Urbanization	

Cite
Withanage, N. C., & Shen, J. (2024). Evaluating the Spatial-Temporal Dynamics of Urbanization in Prefecture Cities of China Using SNPP-VIIRS Nighttime Light Remote Sensing Data. <i>GU J Sci, Part A, 11(2)</i> , 346-371. doi:10.54287/guj.1466745

Author ID (ORCID Number)	Article Process		
0000-0002-0326-7814	Neel Chaminda WITHANAGE	Submission Date	08.04.2024
0000-0003-4318-8405	Jingwei SHEN	Revision Date	29.04.2024
		Accepted Date	06.05.2024
		Published Date	23.06.2024

1. INTRODUCTION

In recent times, urbanization has experienced substantial growth, becoming a notable spatial phenomenon worldwide. According to the UN-Habitat report by 1950, approximately one-fourth of the global population resided in cities (Habitat et al., 2006). As of the present day, that figure has doubled, and currently, half of the world's total population resides in cities (Thapa & Murayama, 2009). The UN World Population Prospect (2019) has reported that by 2030, approximately 57% of the total population of the global south will reside in cities. Spatio-temporal changes in urban growth and related aspects have been monitored and evaluated in various countries and regions using geo-informatics techniques, especially remote sensing coupled with

*Corresponding Author, e-mail: neel@geo.ruh.ac.lk

various machine learning techniques. This approach allows for the derivation of reliable and consistent urban information (Schneider et al., 2010; Zhang & Seto, 2011; Zhou Y. et al., 2014).

Continuous assessment of city growth and geographical patterns is essential for understanding and addressing the exacerbation of escalating socio- environmental issues in urban environments, including traffic congestion, urban crimes, air pollution, and ecological degradation (Thapa & Murayama, 2009). Additionally, understanding the geographical dynamics in urban land use and land cover (LULC) is vital for long-term resource management perspectives (Wijesinghe & Withanage, 2021; Withanage et al., 2024). In this context, multi-temporal and multi-spectral satellite information serves as an effective source for predicting and simulating urban expansion and growth. Therefore, geo-informatics techniques and tools can play a decisive role in sustainable urban planning initiatives, facilitating a win-win situation for both urban development and environmental conservation efforts (Fan et al., 2014). China has undergone rapid urbanization over the past two decades, leading to a diverse array of socio-environmental issues. Consequently, urban and regional planning authorities are actively seeking effective and reliable measures to overcome and mitigate the negative outcomes associated with the urbanization process. According to statistics from the population census in 2010, nearly 50% of the total population in China resided in cities (Lu et al., 2014). As urbanization rapidly progresses in China, farmlands and other land use classes in countryside areas surrounding urban areas are gradually being encroached upon by built-up areas. These land use classes are often delineated from urban areas and commonly referred to as "suburbs" in urban planning and related doctrines (Liu S. et al., 2022). Also, urbanization and sub urbanization have accelerated a diverse array of socioeconomic and environmental issues, affecting both urban and rural environments. Indeed, the demarcation of urban areas and suburbs, coupled with an understanding of their spatial and temporal patterns, plays a pivotal role in achieving sustainable resource management, especially in urban areas in China.

Impervious surfaces in cities are covered by various concrete structures, including roads and other transport networks, a diverse range of buildings such as houses, industrial plants, and other man-made structures that overlay the natural landscape (Zhou Y. et al., 2014; Zhang X. et al., 2020). The MODIS, Sentinel, and Landsat remote sensing images are commonly utilized to detect the geographical dynamics of impervious surfaces in cities. Indeed, evaluating only these structures does not provide an accurate picture of the urbanization process and dynamics. Assessing only these physical structures is inadequate for understanding the geographical evolution of human activity surfaces in the complex urban environment (Ellison et al., 2010). Because of the complex nature of human activities and land utilization in cities, relying solely on changes in impervious structures using multi-source remote sensing data is inadequate for urbanization monitoring (Grove et al., 2015). Indeed, Operational Line-scan System (OLS) nighttime light (NTL) images from the Defense Meteorological Satellite Program (DMSP) and the Suomi National Polar Partnership Visible Infrared Imaging Radiometer Suite (SNPP-VIIRS) NTL data provide a unique proxy for measuring urban dynamics, as they capture both impervious surfaces and human activity surfaces based on NTL brightness value (Imhoff et al., 1997; Xu et al., 2014).

In recent years, monitoring of urbanization and related phenomena, including city size dynamics, spatial structures, and the effect of urban growth on CO₂ emissions, has been a primary focus of research using nighttime light data in China. Most researchers have evaluated urban expansion using stable NTL data, while some have attempted to introduce correction techniques to improve the reliability of their assessments (Elvidge et al., 2009; Zheng et al., 2021). Past scholars have utilized a new generation of NTL data as well as new methods and techniques for urban area delineation and extraction (Liu Z. et al., 2012; Ma T. et al., 2012; Fan et al., 2014; Xu et al., 2014). Those methods included neighborhood statistics, NDVI, and local-optimized thresholds, which were used to extract urban areas based on pixel brightness variations of NTL images (Xiao et al., 2014; Ma T et al., 2015; Su et al., 2015; Shi et al., 2016). Another focal technique used by some researchers was k-means classification to extract built-up areas (Lin et al., 2019; Shi et al., 2023; Withanage et al., 2023). In their analysis, Tian and Qian (2021) endeavored to address the challenge of accurately identifying suburbs in China by leveraging multi source data and integrating multi-logistic regression (MLR) with geographically weighted regression techniques. Furthermore, Feng et al. (2020) employed a k-means algorithm to develop a methodology for delineating the urban-rural fringe in Beijing city, utilizing DMSP/OLS NTL data. Sun and Zhao (2018) endeavored to quantify and compare urban expansion across 13 cities within the Jing-Jin-Ji Urban Agglomeration. They scrutinized the relationship between urban structure and growth

from 1978 to 2015, uncovering considerable variations in expansion patterns attributable to political and other socioeconomic influences. Tian (2020) delineated the suburbs of Jiangsu by estimating spatial interactions through a regression model and a radiation model, evaluating such interactions at a grid level. Consequently, the suburban expansion of Jiangsu over the span of 20 years was found to be noteworthy. Dai et al. (2021) assessed the spatial mutation characteristics of the urban fringe area in Jiangyin city, China by integrating multi-index fusion and wavelet transform techniques. They corroborated their findings by comparing them with results derived from other studies employing the information entropy model and the comprehensive index model. Huang et al. (2020) introduced a quantile method to extract the structure of urban-suburban-rural areas utilizing consistent NTL data from DMSP/OLS. They applied this approach in the Beijing-Tianjin-Hebei region of China using the NTL threshold. Jia et al. (2021) employed an urban-rural gradient approach to investigate the impact of urbanization on land surface phenology across 343 cities in China. They utilized VIIRS Land Surface Phenology in conjunction with MODIS Land Surface Temperature (LST) products for their analysis.

As the k-means algorithm was not commonly applied for delineating urban areas in complex urban environments, we have utilized it as a novel method for extracting both urban and suburban areas in China. This effort assessed the reliability and effectiveness of SNPP-VIIRS-like and SNPP-VIIRS NTL data for urban area identification, addressing this identical flaw. Using both datasets, we aimed to extract and evaluate the geographical dynamics of cities and suburban areas in both provincial and prefecture-level cities using data spanning the period from 2000 to 2020. We structured this paper into five sections. Section one is dedicated to the introduction, encompassing the rationale, objectives of the study, and literature survey. Section two describes the materials and methods, along with the study area description. The third section focuses on the results, with two subsections including urbanization and suburbanization in China. Section four delves into the discussion, comprising the role of SNPP-VIIRS data for urban mapping, the relationship between urban growth and socioeconomic growth, as well as limitations and future research focus. The final section is the conclusion.

2. MATERIALS AND METHODS

2.1. Study Area

China ranks as the world's fourth-largest country by land area, boasting diverse and extensive landscapes, climates, and ecosystems. Spanning from approximately 73.5°E to 135°E longitude and 4°N to 53.5°N latitude it encompasses a wide territory that showcases a wide range of geographical features and environmental conditions. The Country is bordered by the rugged terrain of the Himalayas and the Tibetan Plateau to the west. In the central and eastern regions, it features fertile plains, including the Yangtze River basin. The country also features diverse climatic zones, ranging from arid and semi-arid regions in the northwest to humid subtropical and tropical climates in the south. The country hosts maritime resources and shipping routes along its coastline, which stretches over approximately 18,000 km along the Pacific Ocean.

Urbanization in China has been a significant phenomenon, featuring accelerated growth and transformation. Over the last few decades, millions of people have migrated from the countryside to urban centers in search of better economic opportunities and lifestyles. This great migration has led to the growth of cities and the development of new cities across the country. Several causes have contributed to the rapid urban growth, including industrialization, economic reforms, and government policies aimed at promoting urban development. As a result, China now has some of the largest and most populous cities in the world, such as Shanghai, Beijing, and Guangzhou. As of 2021, the urbanization rate in China stood at 63.8%. In 2016, urban and suburban areas occupied approximately 2.15 million square kilometers, which is equivalent to a considerable portion of the country's total land area (He et al., 2017; Liu S. et al., 2022).

China has been divided into 23 provinces, 5 autonomous regions, 4 direct-controlled municipalities, and 2 Special Administrative Regions (SARs) for ease of administration. Guangxi, Inner Mongolia, Ningxia, Tibet, and Xinjiang are autonomous regions. Beijing, Chongqing, Shanghai, and Tianjin are designated as direct-controlled municipalities. Hong Kong, Taiwan, and Macau are designated as SARs (National Bureau of Statistics, 2021; Withanage et al., 2023). In China, prefectures are administrative divisions that are below the provincial level but above the county level. Prefectures typically encompass several counties. The number of prefectures in China can change over time due to administrative reforms and adjustments. As of January 2022,

there were over 330 prefecture-level divisions. However, our study area is limited to provinces and prefecture-level divisions within mainland China due to data availability constraints. For the study, the selected provinces and prefecture-level cities were categorized into eight groups based on their geographical coverage: east, west, central, south, north, northeast, northwest, and southwest (Figure 1).

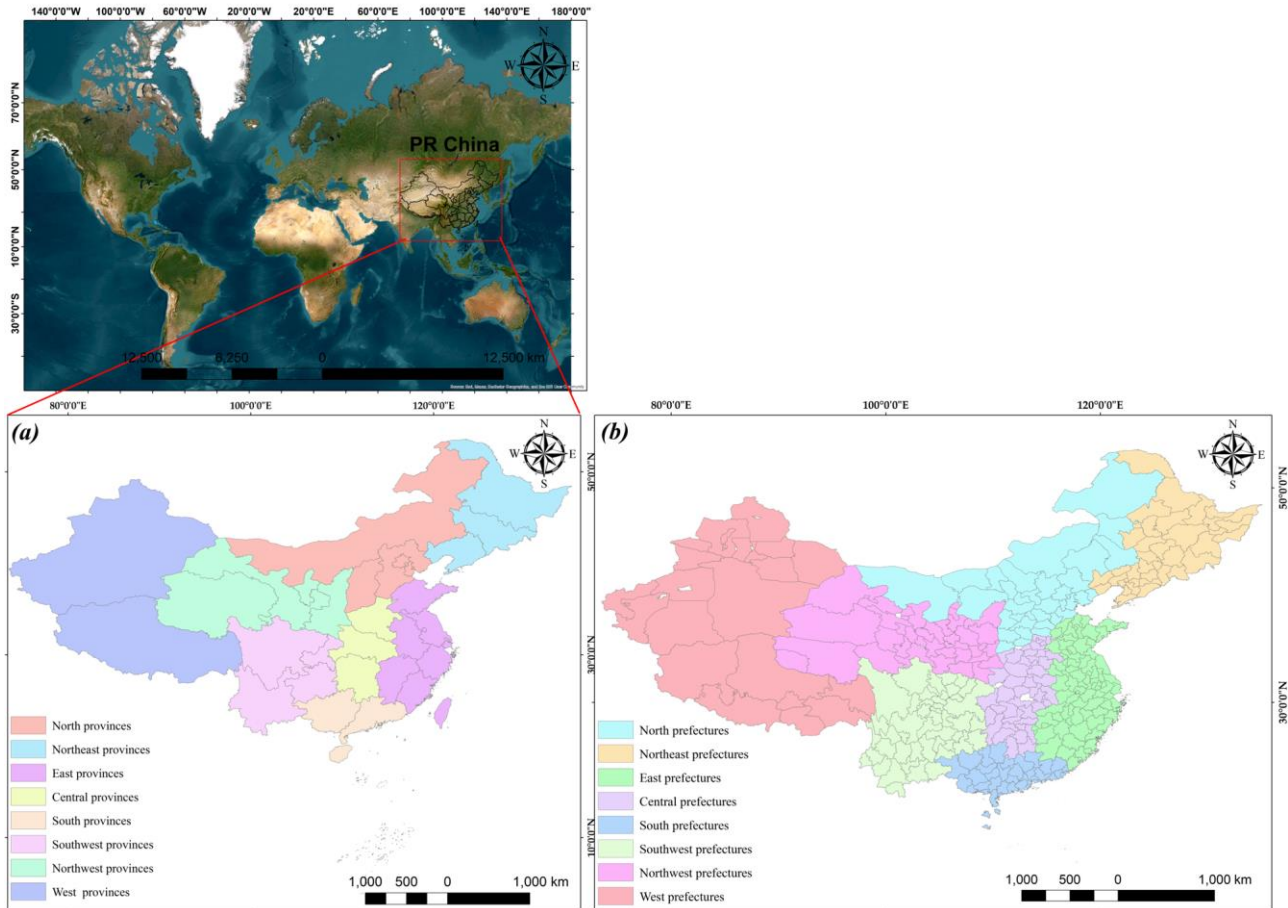


Figure 1. a) provinces in PR China, b) prefecture divisions in PR China

2.2 Materials

Two main spatial data sources were utilized to extract urban and suburban areas: Newly generated SNPP-VIIRS-like data, which covers the period from 2000 to 2023 (Chen et al., 2020). The dataset provides a comprehensive view of NTL emissions and urbanization trends over two decades, facilitating the identification of urban growth trends and changes in human activity and provides valuable insights into NTL emissions and urbanization trends over two decades; SNPP-VIIRS data spanning from 2012 to 2020 (Chen et al., 2021). This dataset offers more recent and detailed information on NTL emissions, enabling researchers to assess urban development and changes in built-up areas over the past nine years. Both datasets are freely available for research purposes from (<https://dataverse.harvard.edu/dataset.xhtml>). SNPP-VIIRS-like data was generated by merging SNPP-VIIRS and DMSP-OLS datasets, providing consistent and prolonged temporal coverage with 1000 m spatial resolution (30 arc second) and SNPP-VIIRS data have a 500 m (15 arc-second) spatial resolution (Liu S. et al., 2022). The shapefile data of national, provincial, and prefecture boundaries was obtained from the National Geomatics Center of China (<http://ngcc.sbsm.gov.cn/>). Collecting data on GDP, population, and electricity consumption (EPC) values at the provincial level from the China Statistical Yearbook is a standard practice in research related to socio-economic analysis and urbanization studies. The City Statistical Yearbook is a comprehensive and authoritative source of statistical data published annually by National Bureau of Statistics (<https://data.cnki.net/>).

2.3 Methodology

2.3.1 Deriving Urban and Suburban Areas

Performing the k-means algorithm in the image classification stage allowed for the segmentation of the datasets into distinct clusters based on nighttime light emissions. This step was essential for delineating urban and suburban areas from the satellite imagery. Various spatial data clustering algorithms, such as threshold, mutation detection, and ordering points to identify the clustering structure (OPTICS), as well as k-means, are at one's disposal. Because OPTICS is sensitive to parameters, it may fail to provide more accurate results when density declines between clusters are not present. Moreover, the mutation detection method exhibits several limitations when it comes to extracting urban areas and boundaries within heterogeneous urban environments. The Threshold method accurately extracts urban areas by considering the differences in brightness values within an image. But, k-means is a prominent algorithm since it can support large datasets, simple processes, and fast-running procedures in the computer system compared to other algorithms (Delmelle, 2015; Li et al., 2015; Yang et al., 2017; Hu et al., 2020; Shi et al., 2023; Withanage et al., 2023). The extraction of urban entities (2000-2020) and suburbs (2012-2020) entailed the utilization of k-means unsupervised classification following the acquisition of two datasets. In the case of urban entity extraction, the algorithm divided the dataset into two classes (urban and non-urban) upon the brightness values. In the context of suburbs, the number of extraction clusters was defined as three, comprising urban, suburban, and rural categories. Additionally, three initial prime centers were randomly selected for the clustering process. Below is the calculation formula (Shi et al., 2023; Withanage et al., 2023);

$$\mu_i^{j+1} = \frac{1}{|C_i|} \sum_{x \in C_i} x \quad (1)$$

$$E_i = \sum_{i=1}^k \sum_{x \in C_i} |x_i - \mu_i^{j+1}|^2 \quad (2)$$

E denotes the minimum square error of a cluster. For the sample x as $C = \{C_1, C_2, C_3 \dots C_k\}$ of the dataset. The similarity among all samples inside the cluster increases when smaller its value. μ_i^{j+1} denotes the center of cluster C_i in the $j+1$ iteration. As the clustering criterion, we used the sum of the square error criterion function, as outlined by Shi et al. (2023) and Withanage et al. (2023).

$$J_C = \sum_{i=1}^k \sum_{P \in C_i} \|P - M_i\|^2 \quad (3)$$

In cluster C_i p denotes all pixels in the cluster, arithmetic mean of all pixels in C_i denotes by M_i . Mapping between cluster centers and data objects represented by J_C . The urban and non-urban feature types of each pixel within an image are identified through cluster analysis. After running the algorithm iteration, urban, suburban, and rural areas were discerned from the two datasets on the variations of color.

2.3.2 Image Post Processing

Following the image classification stage, image post-processing techniques were applied to enhance the reliability and accuracy of the derived urban and suburban outputs. These techniques included noise reduction, and spatial filtering to refine the classification results and remove any inconsistencies. We performed image post-processing techniques to ensure the logical consistency of the extracted urban areas and suburban features. Here we followed three main steps: iterative temporal filtering, logical reasoning, and the elimination of unreasonable urban features (Shi et al., 2023; Withanage et al., 2023). This approach aimed to derive more precise and reliable results both in spatial and temporal dimensions.

2.3.3 Accuracy Assessment

Accuracy assessment involves comparing the classified urban and suburban areas to evaluate the reliability of the classification method and outputs. To assess the reliability of urbanization and sub urbanization pixels produced by the k-means algorithm, We computed accuracy of classification for each class over the pertinent

years. Four commonly utilized accuracy metrics were calculated: Overall Accuracy (OA), Producer’s Accuracy (PA), User’s Accuracy (UA), and Kappa Coefficients. OA stands for the overall percentage of correctly classified pixel classes, which is computed by dividing the number of accurately classified urban and non-urban pixels by the total number of pixels in the datasets (Zhou Q. et al., 2008; Yuh et al., 2023) and can be represented is as;

$$OA = \frac{1}{N} \sum_{ii=1}^n P_{ii} \tag{4}$$

OA stands for overall accuracy while N is total samples number and n denotes the total categories number, and P_{ii} is correct classifications number of *i*th sample. PA measures the percentage accuracy of individual classes within a map. It’s calculated by dividing the number of correctly classified pixels in a specific class by the total number of pixels belonging to that class in the reference data. The calculation formula is as;

$$PA = \frac{\text{Correctly classified number pixel in each category}}{\text{Correctly classified total number pixels in that category(column total)}} \tag{5}$$

UA, assesses the reliability of a given pixel class by evaluating its agreement with ground observations. It’s also calculated by dividing the number of correctly classified pixels in a specific class by the total number of pixels classified within that class as below;

$$UA = \frac{\text{Correctly classified number pixel in each category}}{\text{Correctly classified total number pixels in that category(row total)}} \tag{6}$$

The Kappa Coefficient indicates the level of agreement between test and validation data in generated maps. It’s based on the probability of the test data closely matching the validation data during the urban area extraction process and is highly correlated with overall accuracy. Overall mean accuracy and Kappa values for the urban features were within acceptable ranges as from 0.80 to 0.92% for OA and from 0.75 to 0.88 for Kappa (Table 1). For suburbs, the identification accuracy, measured by OA, ranged from 0.77 to 0.84, while Kappa coefficients ranged from 0.77 to 0.86 for selected years (Table 2).

Table 1. Overall mean accuracy for urban entity identification

Year	2000		2005		2010		2015		2020	
	OA	Kappa								
	0.84	0.80	0.80	0.75	0.92	0.81	0.80	0.82	0.88	0.88
	PA	UA								
Urban	0.82	0.79	0.79	0.74	1.00	0.93	0.79	0.86	0.92	0.91
Non-urban	0.87	0.82	0.81	0.76	0.84	0.88	0.82	0.78	0.84	0.85

Table 2. Overall mean accuracy for suburban area identification

Year	2012		2014		2016		2018		2020	
	OA	Kappa								
	0.84	0.77	0.78	0.79	0.78	0.86	0.80	0.83	0.77	0.80
	PA	UA								
Sub-urban	0.79	0.81	0.78	0.79	0.82	0.84	0.77	0.75	0.74	0.73
Urban	0.82	0.77	0.76	0.74	0.76	0.81	0.80	0.81	0.79	0.82
Rural	0.93	0.74	0.81	0.85	0.78	0.94	0.83	0.94	0.80	0.86

3. RESULTS

3.1 Urbanization in China

Statistically significant positive trends in digital number values of NTL images in the prefecture-level cities indicated that China has experienced rapid urban growth from 2000 to 2020 (Figure 2). The highest rate of urban growth could be identified in the five national-level agglomerations: Pearl River Delta (PRD); Beijing-Tianjin-Hebei; Yangtze River Delta (YRD); Middle Yangtze; and Chengdu-Chongqing. Variations in DN values in SPNS VIIRS-like imagery reveal greater changes in urbanization, particularly in the eastern region of the country, from 2000 to 2020.

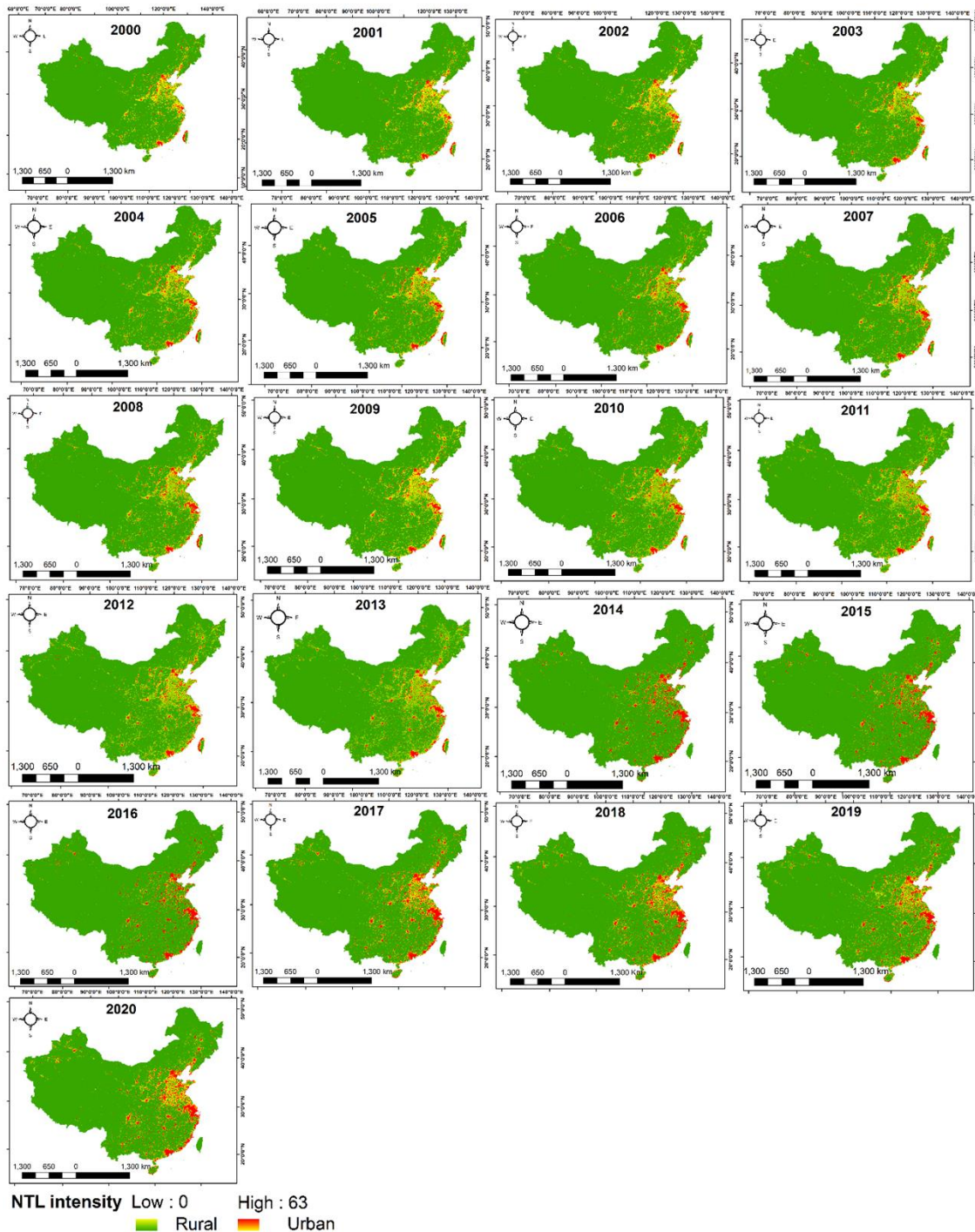


Figure 2. Urban Growth in China, 2000-2020

Based on the variations in DN values in SPNS VIIRS imagery, significant changes in urbanization are notably evident, particularly in the eastern region of the country, from 2000 to 2020. The DN values of inter-calibrated SNPP VIIRS NTL signals in the prefecture cities indicate a substantial inverse pattern into enhanced light areas in cities. Varied spatial and temporal trends in urban entities may suggest that light signals from NTL images could be a marker of urban expansion during significant urbanization in China at the prefecture level. Based on Figure 2, the brightly illuminated areas (highlighted in red with DN values >56 in this case) likely represent the developed sections of cities with dense human activities and a high percentage of impermeable surfaces. The yellow areas, which are moderately to highly illuminated, seem to be associated with the outskirts of the central area and suburban regions with significant human activity. The green areas, characterized by low nighttime lighting, mainly cover rural areas with farmland and small communities with low human activity. Most prefecture cities with well-developed urban areas and human activities have shown a significant positive trend in highly illuminated areas at the city level, indicating significant growth outward from the core region and an increase in the spatial extent of urban entities. However, during the period in concern, notable spatial variations in the expansion of urban entities can be observed across distinct regions (Figure 3).

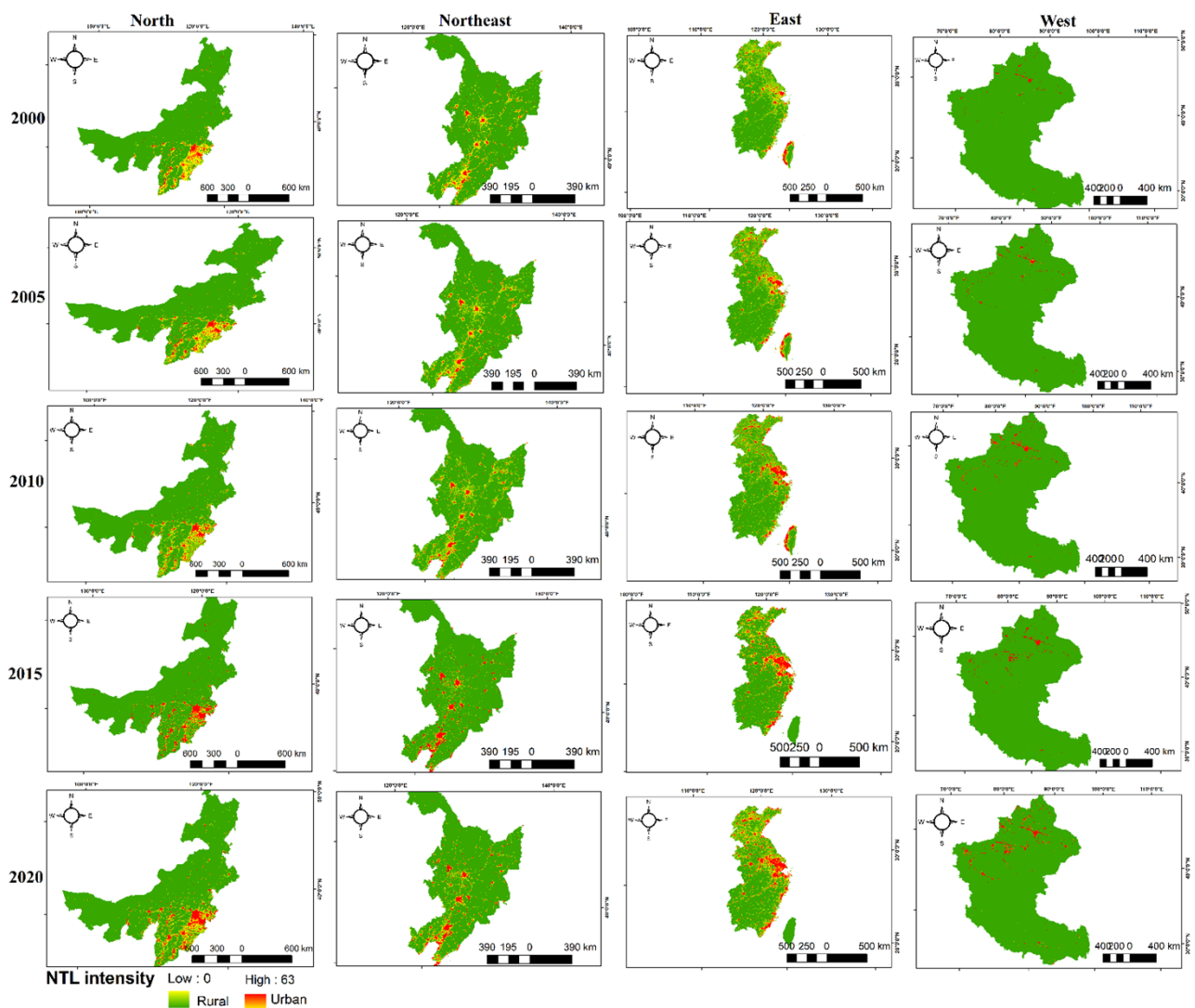


Figure 3. Expansion of urban areas in China during 2000-2020

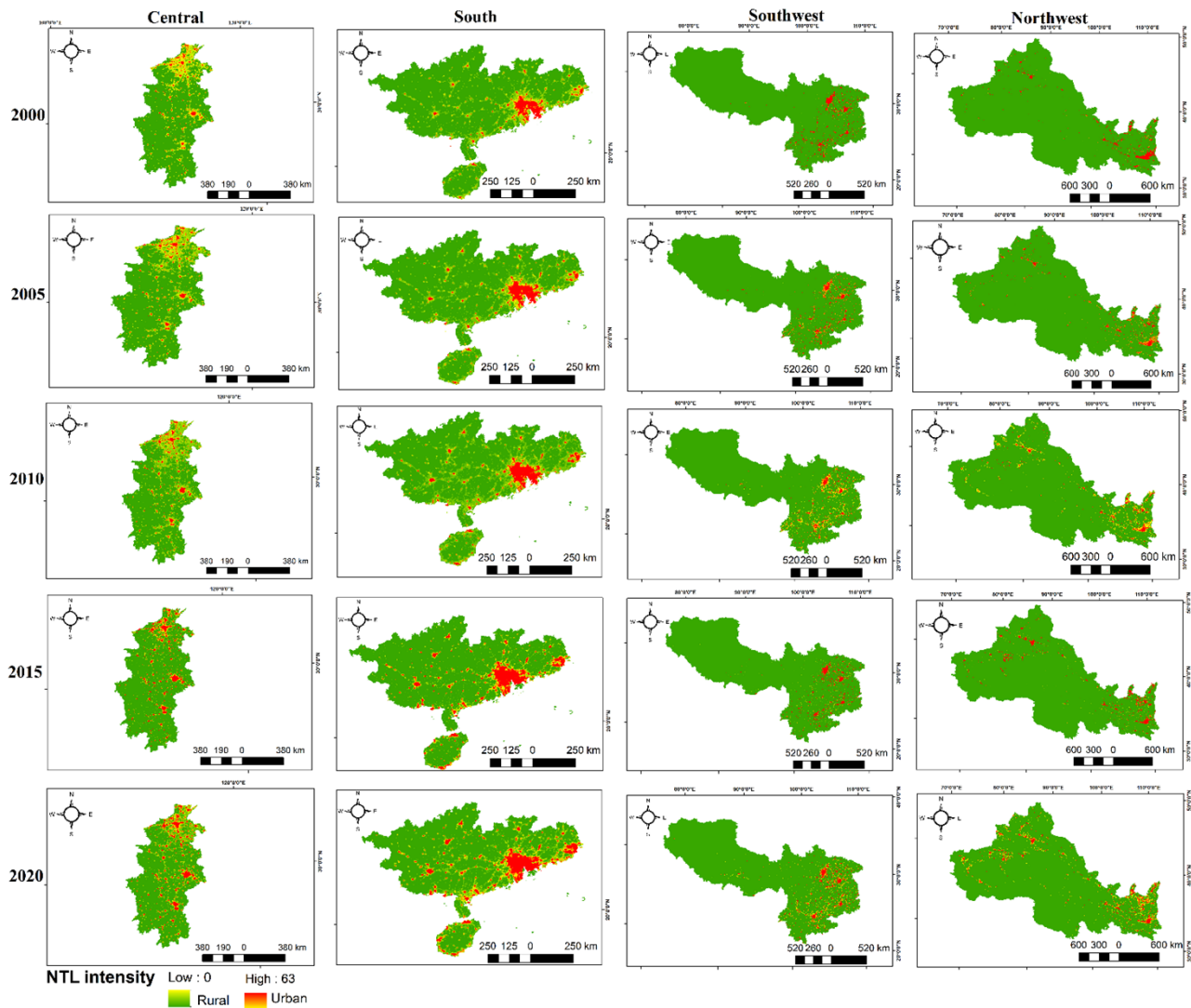


Figure 3. (continued)

3.2. Spatial Variations in Regional Scale

At the individual urban scale, especially most large and extra-large cities in the southern and eastern regions have experienced a distinct reduction of the areas with low NTL over the concerned period, while expanding high NTL areas. The eastern region has demonstrated a notable expansion compared to others, driven by socioeconomic factors and other forces of urban growth. This region includes the Yangtze River Delta (YRD) agglomeration.

The Beijing–Tianjin agglomeration (Figure 4a) has experienced a notable expansion during the last two decades in its geographical scope, accompanied by a heightened level of economic activity. From 2000 to 2020, the total urban entity of the agglomeration increased from 2438 km² to 12,970 km², indicating an average annual growth rate of 21.6%. During the specified period, the Beijing–Tianjin agglomeration exhibited a contrasting trend to the growth observed in the YRD, showing a decline in urban sprawl.

The Chengdu–Chongqing agglomeration (Figure 4b) sits in the Southwest sector of China, situated upstream along the Yangtze River. The collective urban entity within the region saw an increase from 204 km² to 5036 km², reflecting an average annual growth rate of 118.4%. This agglomeration spans approximately 185,000 km² and includes 15 prefecture-level cities in Sichuan Province and 29 district/county-level administrative units in Chongqing Province. With an urbanization rate of 63.01% among its permanent population, this agglomeration stands as a pivotal demonstration area for the nation's advancement of new urbanization (Luo et al., 2023).

As a key agglomerations for development, the YRD (Figure 4c) encompasses Shanghai, Jiangsu, Zhejiang, and Anhui provinces, comprising fifty-one cities, including 26 prefecture cities, including Shanghai (Anhui 8, Zhejiang 8, Jiangsu 9), covering about 225,000 km² (Zhang H. et al., 2022). The urban entities in all prefecture cities in the eastern provinces have significantly expanded, including provincial capitals like Shanghai, Hangzhou, Fuzhou, Jinan, Nanchang, Nanjing, and Hefei. The urban entities within the YRD region expanded significantly from 2684 km² to 41465 km² between 2000 and 2020, indicating an annual average growth rate of 72.2%. As a key urban centre in the Eastern region Shanghai has risen greatly from 660 km² to 2852 km² demonstrating a 45% growth rate. Land urbanization is more pronounced in the southeast prefectures of the YRD agglomeration compared to those in the northwest. Higher levels of land urbanization have occurred over the specified period, particularly in the core areas of Shanghai, Nanjing, and Hangzhou, as depicted in the Figure 4c. Nevertheless, land urbanization in certain mountainous prefectures in southern Anhui and Zhejiang has shown a low level of development.

During the specified period, prefecture cities in southern provinces experienced significant growth, with a notable expansion observed in those within the Pearl River Delta (PRD) urban agglomeration (Figure 4d). The urban entity in the Pearl River Delta (PRD) increased from 4147 km² to 12,962 km², illustrating a growth rate of 213%. Despite comprising only 0.58% (56,000 km²) of the total land area, the PRD urban agglomeration significantly contributes to 9.2% of the GDP (Zhang H. et al., 2022). Among the seventeen cities in the PRD, nine prefectures serve as crucial urban hubs in the region. These include Guangzhou, Shenzhen, Zhuhai, Foshan, Jiangmen, Zhaoqing, Huizhou, Dongguan, and Zhongshan. Based on the NTL imagery retrieval data, Shenzhen, situated in the southern part of the PRD, has exhibited significant growth in urban development from 2000 to 2020. Following closely behind is Guangzhou, which is the second most rapidly expanding urban entity in the region. Nevertheless, several adjacent cities, such as Zhaoqing, Huizhou, and Jiangmen, have shown relatively modest urban growth over the specified period.

3.3 Spatial Variations in Prefecture Scale

During the specified period, the total urban entity in mainland China expanded from 16,209 km² to 89,631 km² indicating a growth rate of 5% during the last 20 years. However, the rates and patterns of growth in urban entities (UEs) exhibited significant variations across eight regions undergoing diverse economic and urban development stages. The eastern and southern prefectures contributed the highest growth in urban expansion, with 27,640 km² and 9,340 km², respectively, while the northeast and northwest prefectures showed lower spatial extents of 2,897 km² and 5,207 km², respectively.

Shanghai, located in the eastern prefectures (Figure 5), has experienced dramatic growth over the last 20 years, expanding from 660 km² to 2,852 km² (Figure 5y). As fast growing prefecture in the southern provinces, Guangzhou expanded its urban area from 375 km² to 1,635 km² (Figure 5v). In Beijing, urban areas expanded from 783 km² to 2,150 km², making it the fastest-growing prefecture in the northern regions (Figure 5q). From a temporal perspective, certain provincial capitals like Chongqing and Chengdu exhibited rapid expansion after 2015 (Figure 5m, n). However, some provincial capitals like Xining, Lhasa, Haikou, and Hohhot have demonstrated comparatively slower spatial expansion during the target period (Figure 5h, l, x, u). The temporal patterns and trends of the 31 provincial capitals growth has illustrated in Figure 6.

3.4 Growth of Suburbs

Over the past two decades, significant spatial and temporal changes in land use have occurred in suburban areas, acting as bridges amid urban and rural areas. The k-means method was utilized to discern and assess the spatial-temporal patterns of sub-urbanization in China mainland using SNPP VIIRS data from 2012 to 2020. The suburbs underwent a proportional expansion attributed to factors such as population density, urban GDP growth, and the development of the road network. The analysis revealed that the overall area of suburbs expanded from 59,151 km² to 120,339 km² between 2012 and 2020 (Figure 7), indicating a proportional growth rate ranging from 0.6% to 1.2%. The peak growth rate of suburbs was recorded between 2012 and 2014, reaching 18%. Urban areas and suburbs experienced integrated growth during the specified period, with both entities mutually benefiting from each other for their area growth. Consequently, the spatial and temporal urban-suburb development sequences are accurate. Figure 8 illustrates the proportions of suburbs and urban

entities in the years 2012, 2014, 2016, 2018, and 2020. Figure 8 demonstrates a notable increase in the proportional contribution of suburbs compared to urban entities.

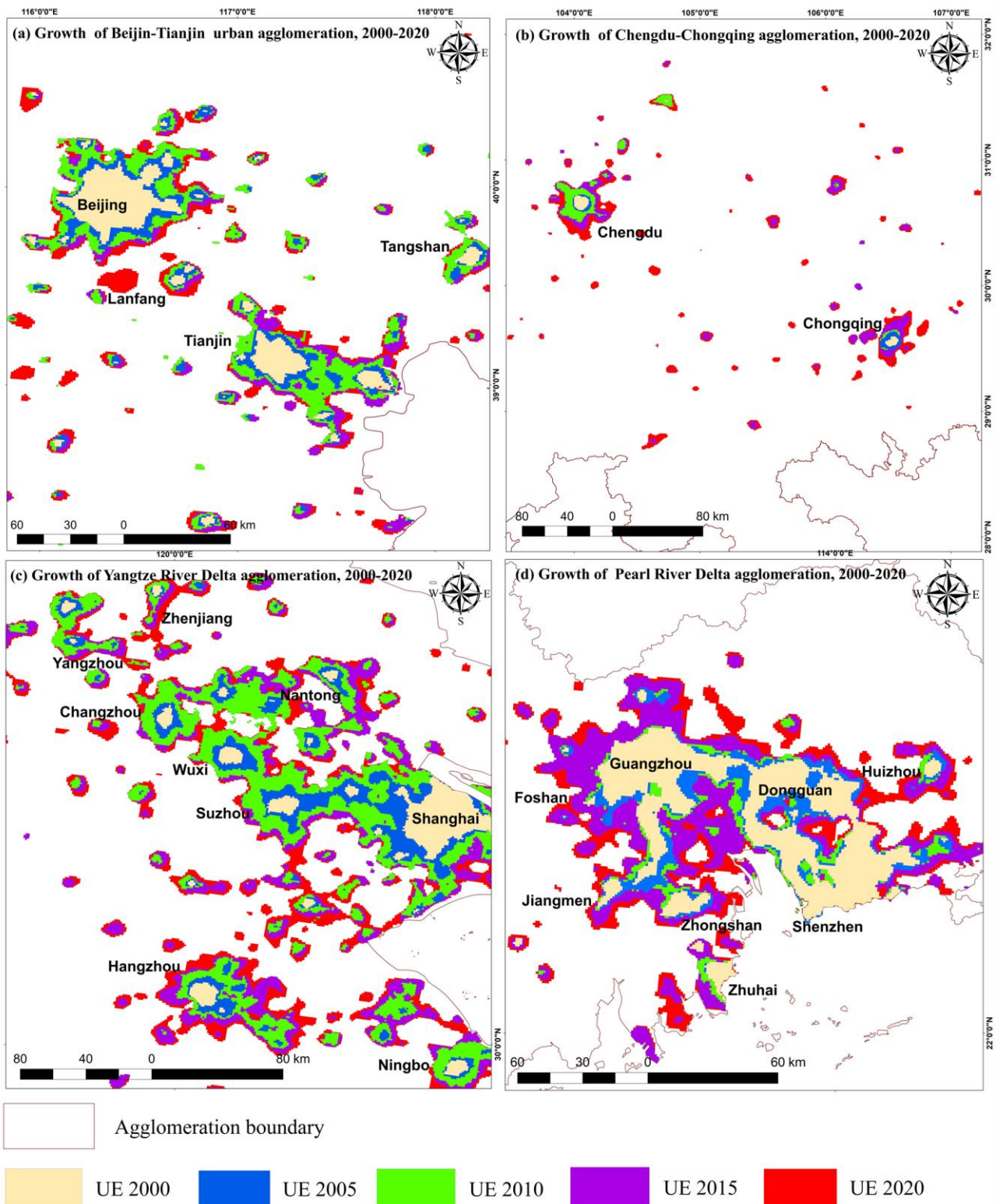


Figure 4. Growth of urban entities, 2000-2020 *a)* Beijing-Tianjin agglomeration, *b)* Chengdu-Chongqing agglomeration, *c)* Yangtze River Delta agglomeration, *d)* Pearl River Delta agglomeration

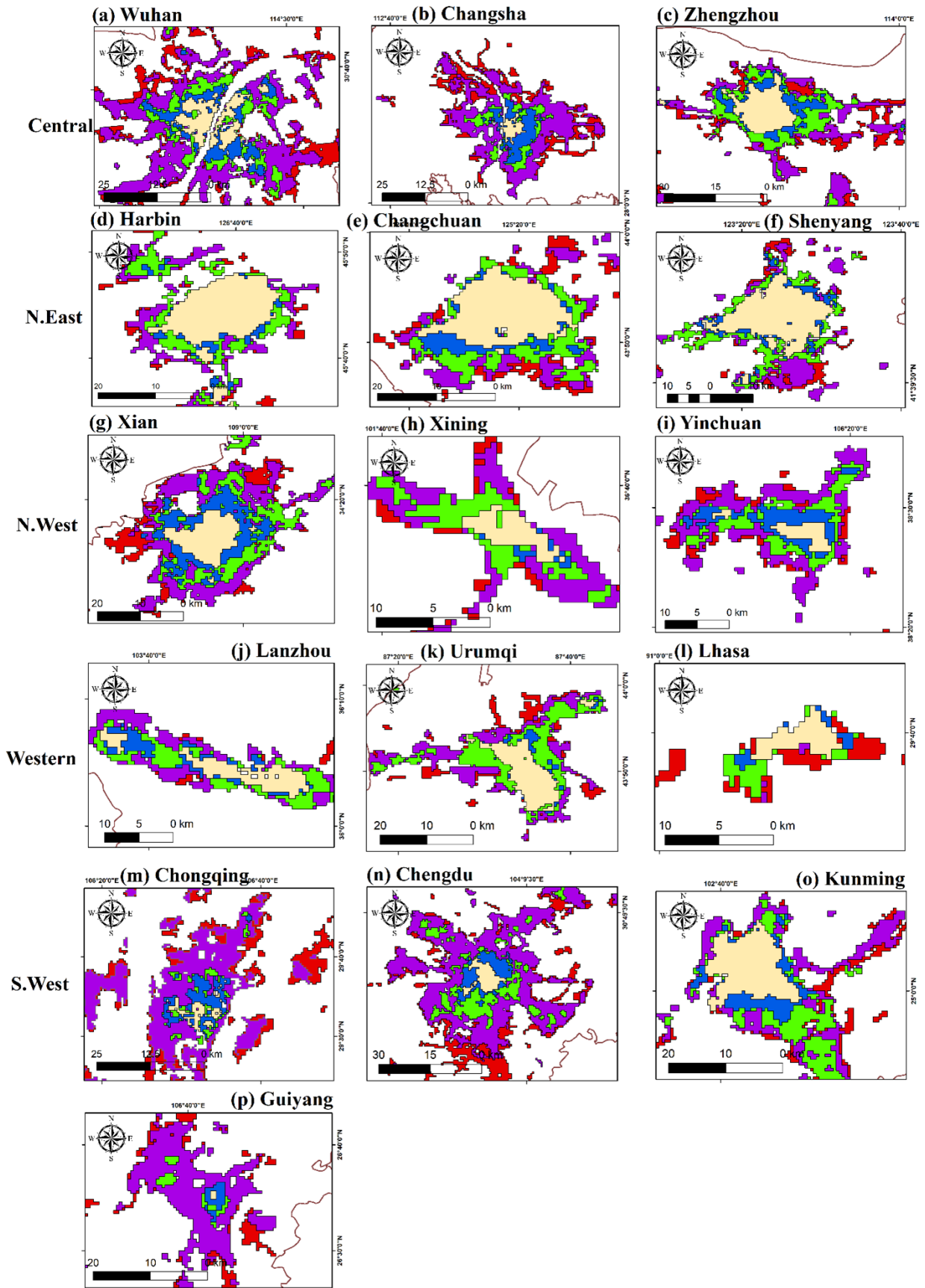


Figure 5. Growth of provincial capitals, 2000-2020

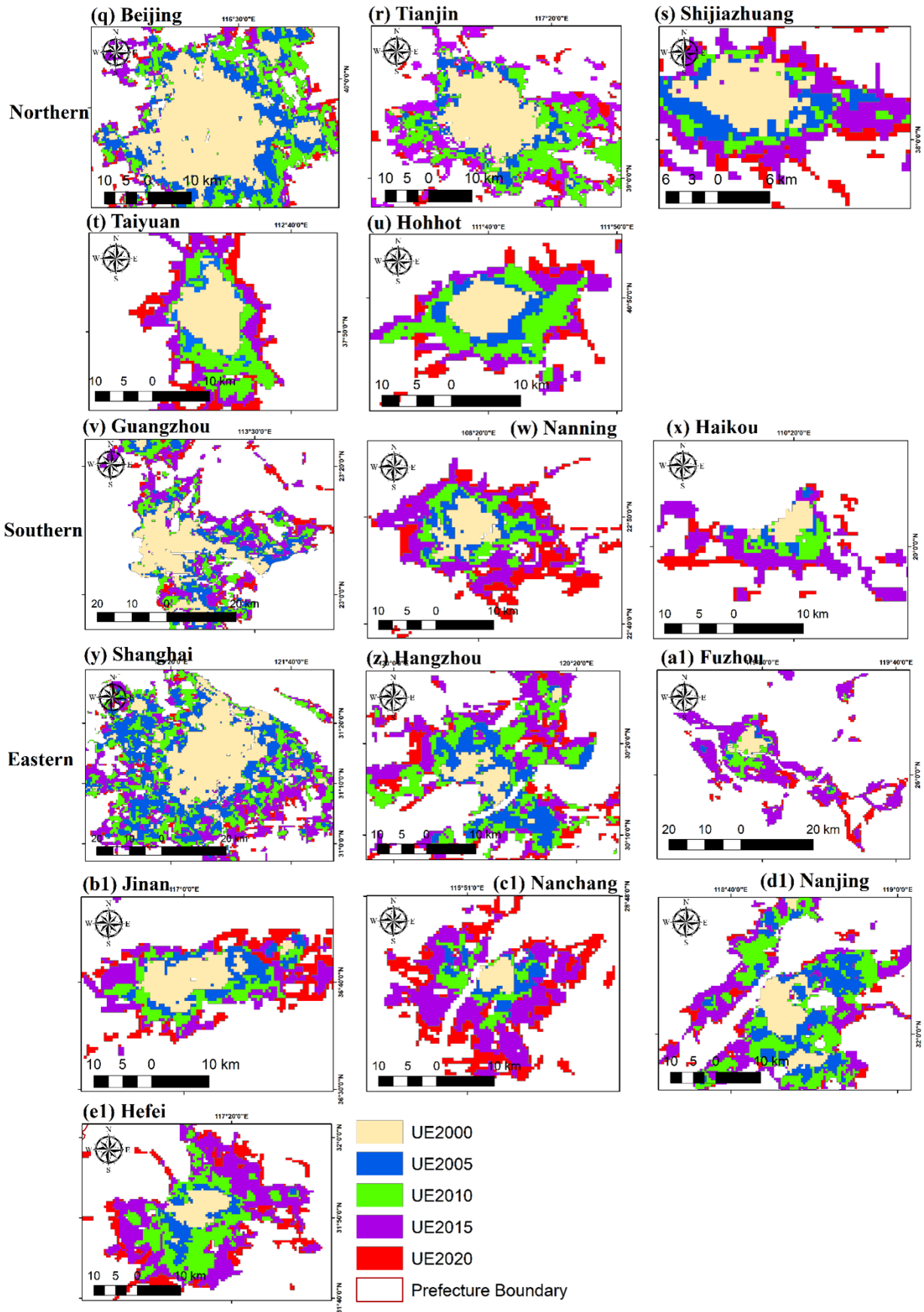


Figure 5. (continued)

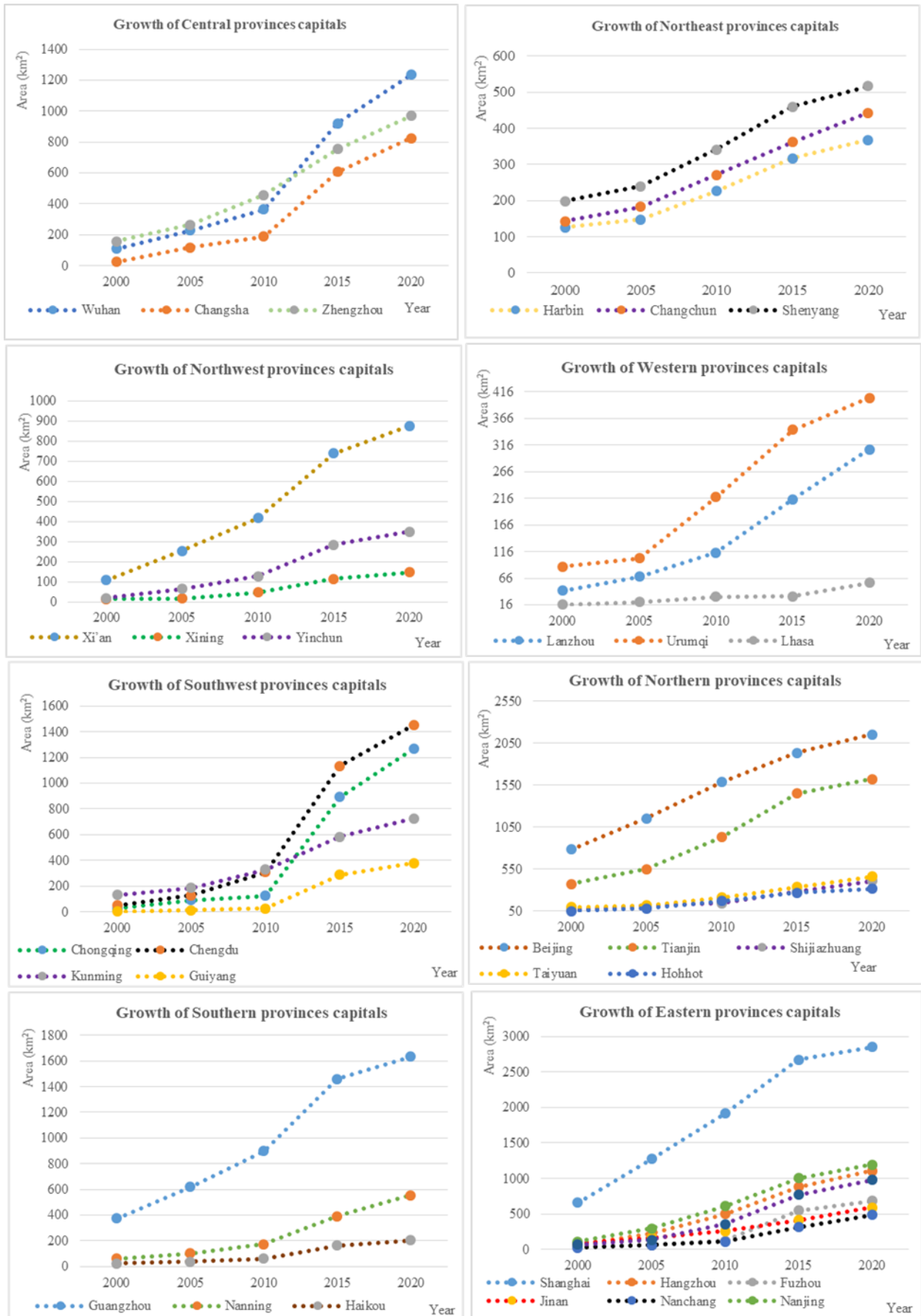


Figure 6. Growth patterns of urban entities in provincial capitals, 2000-2020

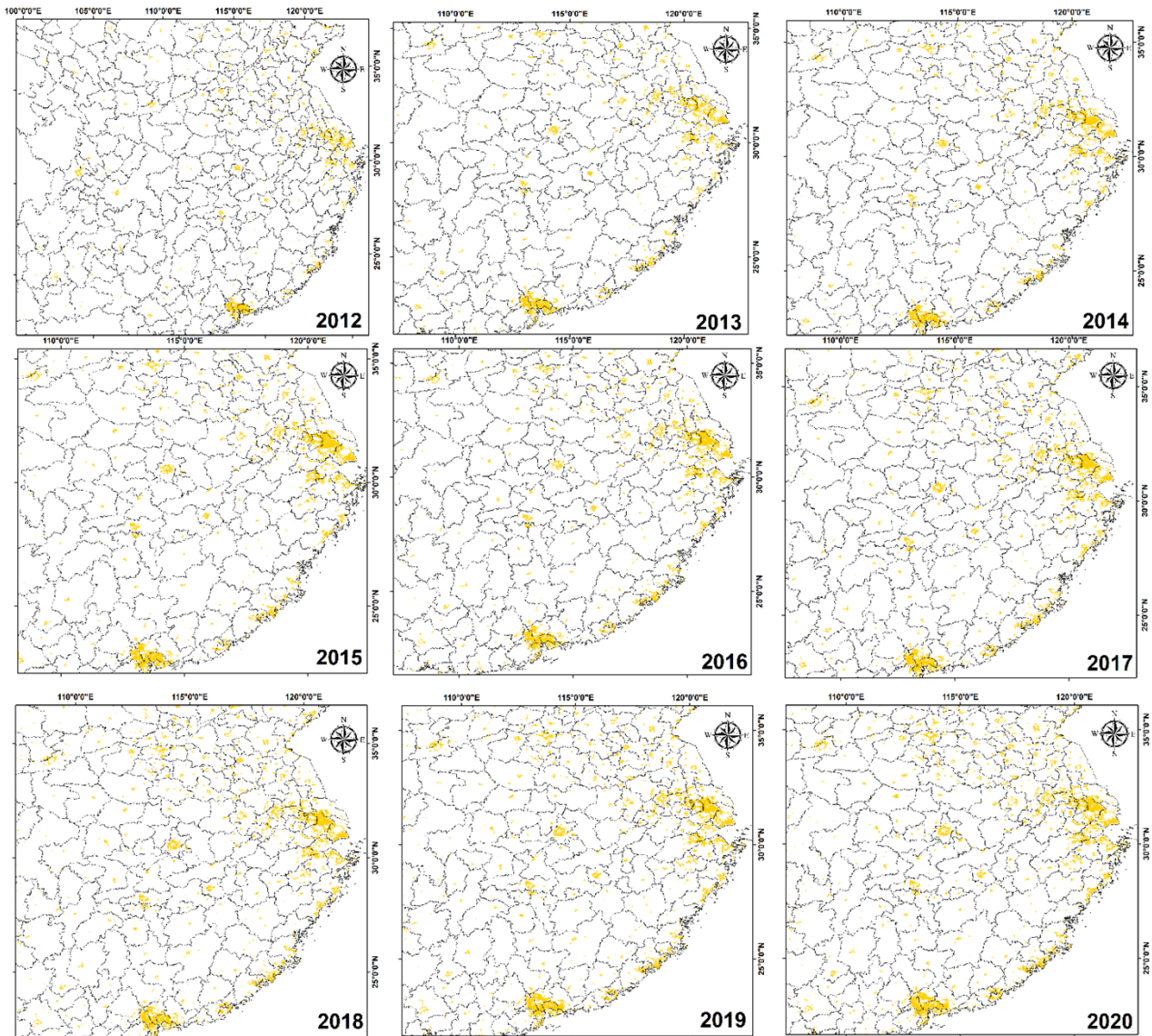


Figure 7. Growth patterns of suburbs in China, 2012-2020

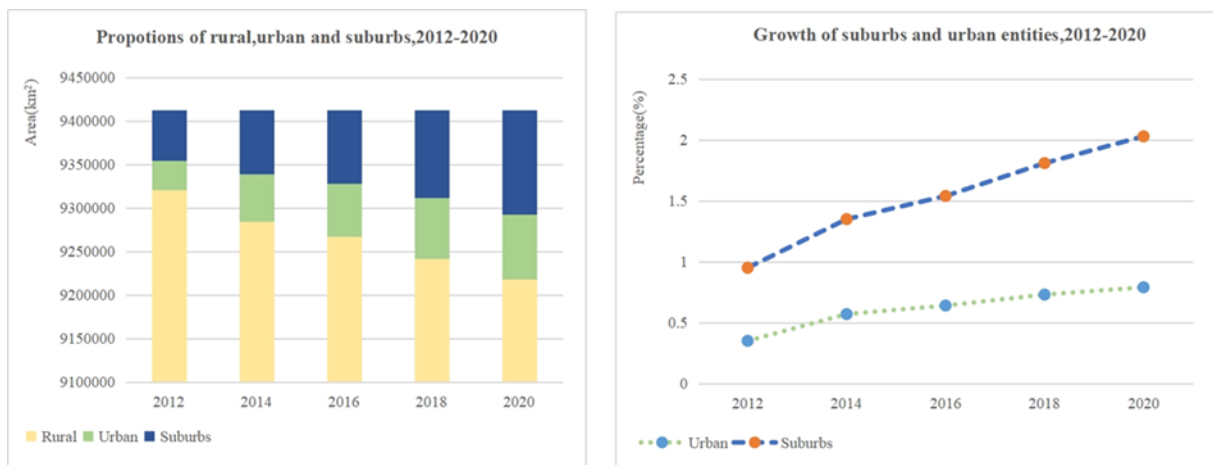


Figure 8. Proportion of rural, urban, and suburbs in China and growth rates of urban entities and suburbs, 2012-2020

When examining the provincial landscape of suburban development, each province exhibits distinct growth trends and patterns. Guizhou, Hunan, and Hubei have exhibited growth rates of 334%, 258%, and 246% respectively throughout the specified period, indicating their status as suburban areas in the intermediate phase of the urbanization process. However, the provinces of Beijing, Guangdong, Tianjin, and Shanghai, which are in the advanced stage of urbanization, have experienced relatively low growth rates of 50%, 56%, 46%, and 17% respectively. This is because these provinces have already established and stabilized as urban areas. Additionally, in Heilongjiang, Liaoning, and Inner Mongolia, slow economic growth has negatively affected urbanization. Thus, the growth rate of suburbs in those provinces is low, with growth rates of 45% and 89% respectively. The spatial and temporal patterns of suburban growth in China can be best illustrated using provincial capitals such as Beijing, Tianjin, Shanghai, Wuhan, Chengdu, Chongqing, Nanjing, Guangzhou, and Xi'an (Figure 9 and Table 3).

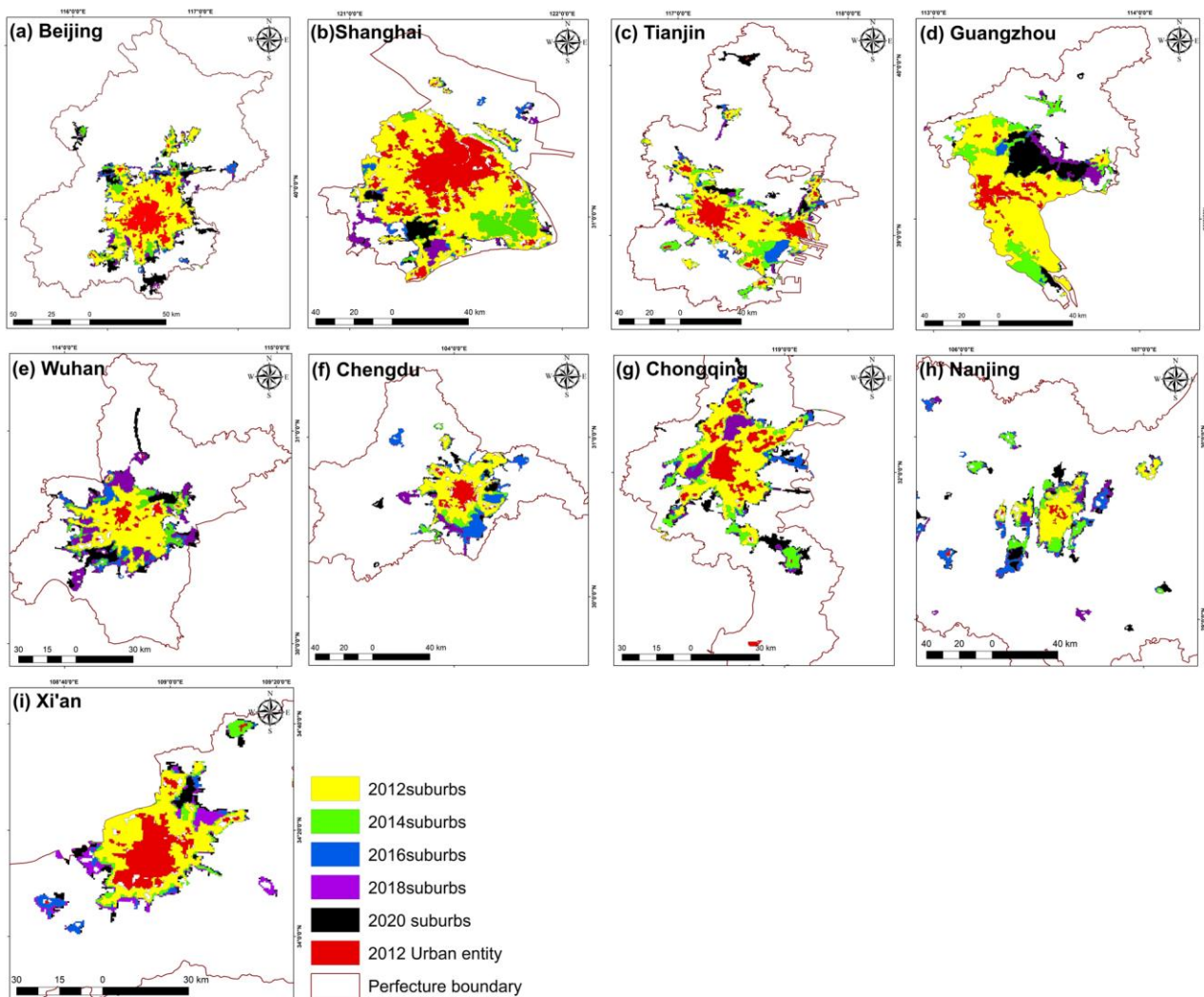


Figure 9. Suburban growth during 2012-2020 **a)** Beijing, **b)** Shanghai, **c)** Tianjin, **d)** Guangzhou, **e)** Wuhan, **f)** Chengdu, **g)** Chongqing, **h)** Nanjing, **i)** Xi'an

Table 3. Top 10 suburbs in the years 2012, 2016, and 2020

City	2012	City	2016	City	2020
	Area (km ²)		Area (km ²)		Area (km ²)
Qingyuan	2103	Suzhou	4119	Suzhou	4363
Shanghai	2074	Shanghai	2390	Guangzhou	2671
Foshan	1869	Guangzhou	2085	Shanghai	2404
Guangzhou	1858	Qingyuan	1988	Foshan	2175
Suzhou	1619	Foshan	1915	Qingyuan	1945
Beijing	1535	Beijing	1697	Tianjin	1718
Tianjin	1171	Tianjin	1639	Hangzhou	1593
Shenzhen	1100	Hangzhou	1390	Wuhan	1528
Hangzhou	975	Wuxi	1310	Chengdu	1457
Chengdu	941	Chengdu	1291	Quanzhou	1394

3.5 Growth Patterns and Driving Factors in Suburb Development

Suburban expansion in cities such as Beijing and Wuhan, it becomes evident that there has been growth in all directions. However, the expansion of Tianjin's suburbs occurred predominantly in a southeasterly direction. Upon analyzing the situation of Shanghai city, it becomes apparent that the suburbs initially expanded on the eastern side. However, thereafter, they expanded in a southern direction. Similarly, the suburbs in Chongqing have been consistently expanding towards the southwest. The suburbs of Guangzhou have experienced a significant trend of northward development from 2012 to 2020. These spatial variations are a result of the effect of several political, economic, and geographical factors. This pattern is better evident from the expansion of suburbs in the Pearl River Delta (PRD).

Therefore, these variables significantly contribute to the process of sub urbanization in China throughout the concerned period. Urban growth in major cities has led to a rise in environmental difficulties such as noise, air, and water pollution in metropolitan regions. As a result, people are increasingly moving from urban areas to suburban areas due to lower land prices and more favorable living conditions. Urban-suburb commuter communities have emerged as a result of the recent growth of road networks and other advantages in suburbs, leading to daily changes. Urban policy making has also significantly contributed to the growth of suburbs in China.

The development of suburbs is closely correlated with the expansion of road networks, population growth, and other socioeconomic development indicators. Provincial-level socioeconomic variables such as Gross Domestic Product (GDP) and Electricity Consumption (EPC) exhibit a higher spatial consistency with sub urbanization according to the regression analysis performed (Figure 10). Observing the R^2 values between population, GDP, EPC, and the suburban area, they were not less than 0.3594, 0.6214, and 0.6252 respectively. According to the regression results among the three socioeconomic variables, higher consistency is exhibited in suburban growth with GDP, as it derived an R^2 value of 0.8758 (Figure 10r). The second-highest R^2 value was reported for EPC as 0.7982 (Figure 10y), while population and suburban area show a comparatively low inverse relationship, reporting an R^2 of 0.6115 as higher (Figure 10i).

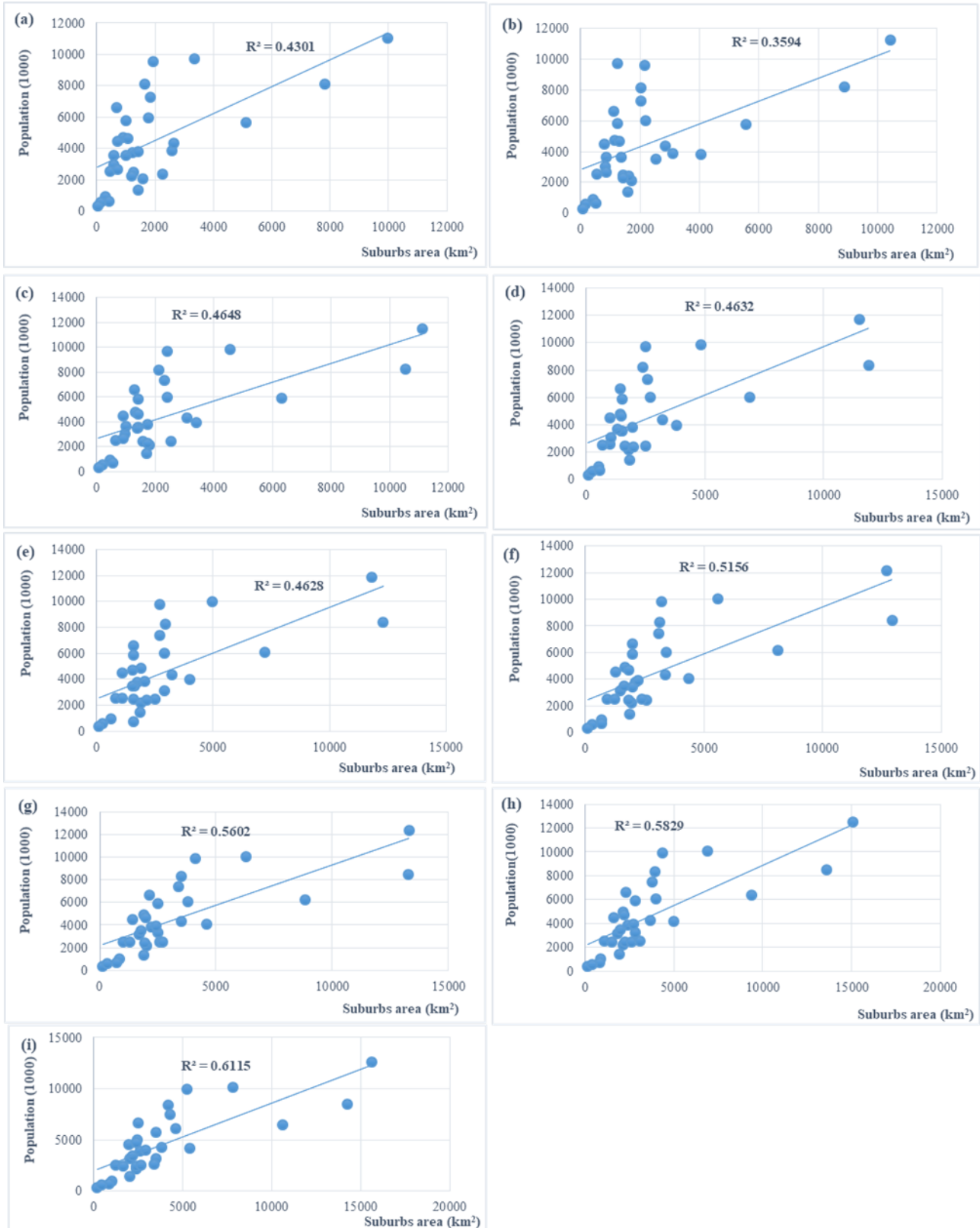


Figure 10. Correlation between the growth of suburban areas and **a-i)** provincial level population, **j-r)** GDP, **s-x1)** EPC

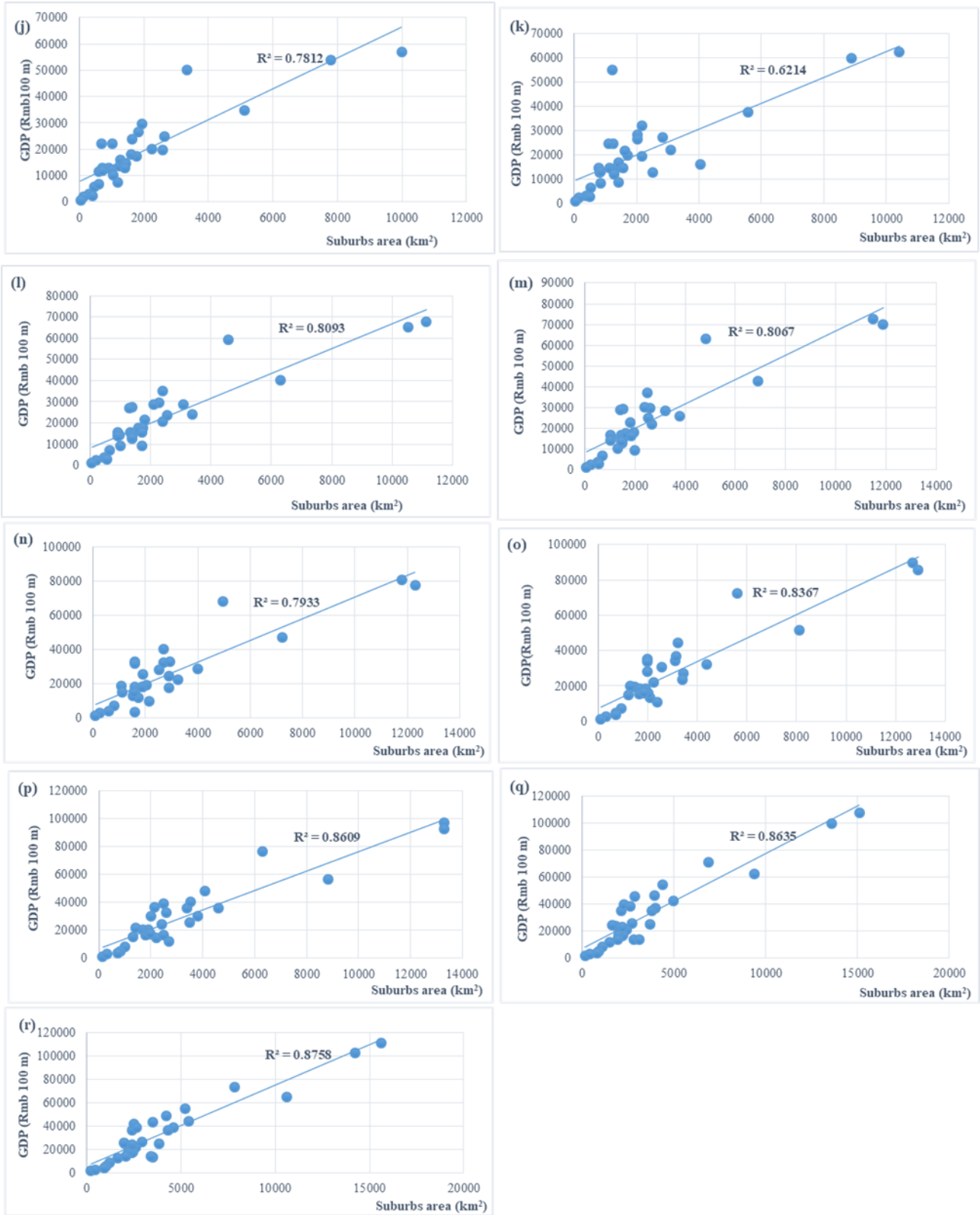


Figure 10. (continued)

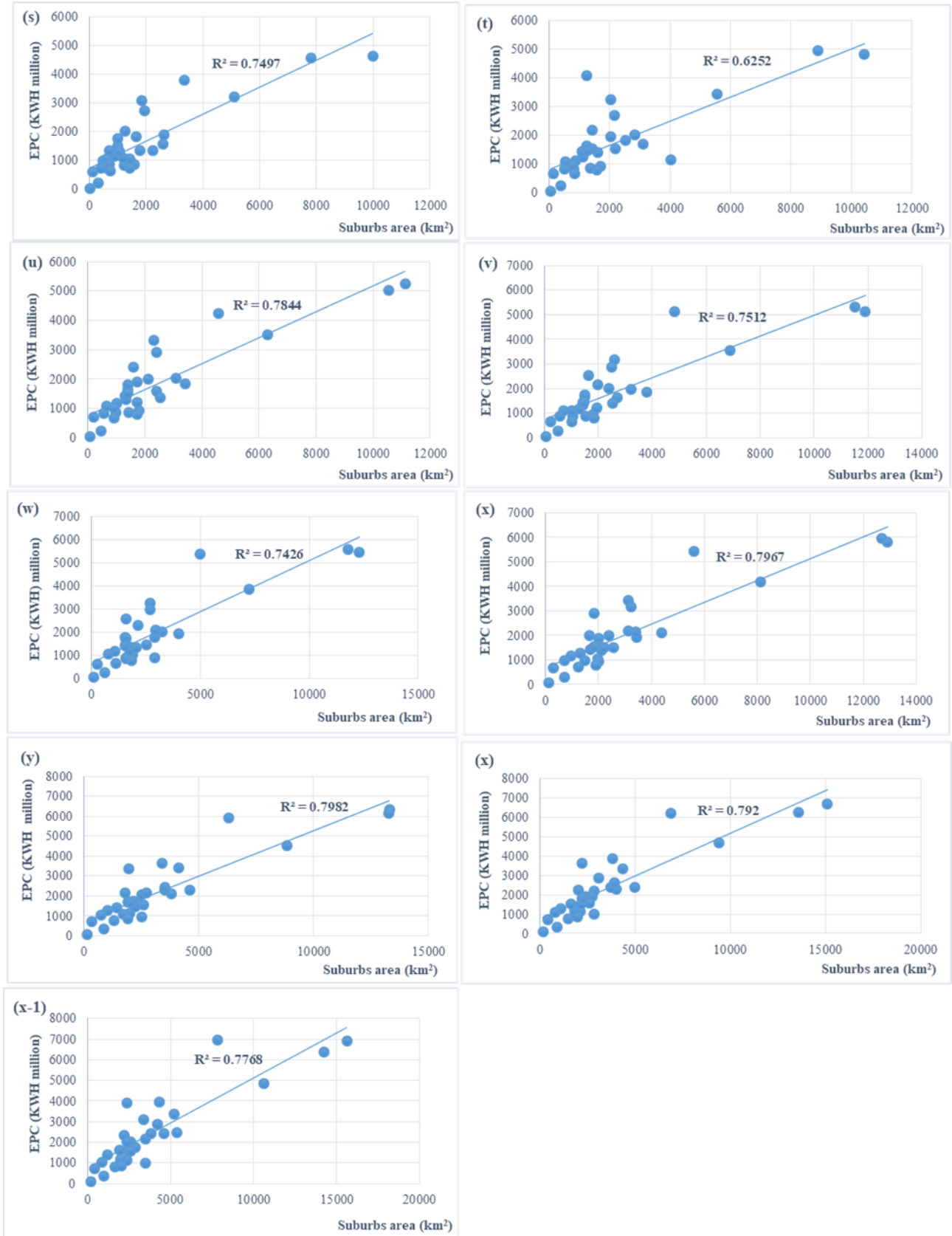


Figure 10. (continued)

4. DISCUSSION

4.1 Role of SNPP-VIIRS Data for Urban Mapping

Demarcating clear urban boundaries solely based on results derived from other remote sensing data such as Landsat and MODIS can be challenging, particularly when considering impervious surfaces. Therefore, it is essential to utilize reliable data that also captures human activity surfaces. Ma M. et al. (2020) demonstrated a positive correlation between nighttime lights and human activity surfaces. We employed the k-means algorithm to extract urban and suburban areas, aiming to evaluate their spatiotemporal evolution using SNPP-VIIRS data. Yu et al. (2018) also confirmed that NTL data is a reliable data source for extracting built-up areas. They revealed that various methods can be employed for reliable urban area extraction, including threshold, watershed segmentation, Sobel-based edge detection, and neighborhood statistics. Shi et al. (2023) and Withanage et al. (2023) similarly employed the k-means method to extract cities utilizing SNPP-VIIRS NTL data. However, Shi et al. (2023) emphasized the importance of integrating NTL data with other sensing data for urban area extraction to attain higher accuracy. Liu S. et al. (2022) have also demonstrated that the results of suburban area extraction derived from SNPP-VIIRS data are more accurate compared to DMSP-OLS. They also revealed that suburban areas have experienced a growth rate from 0.6% to 1.3% from 2012 to 2020, which aligns closely with our findings.

4.2 Urbanization and Socioeconomic Development

Through our correlation analysis, it was discovered that there exists an almost inverse relationship between urban growth and urban socioeconomic indicators. Our findings revealed a higher R^2 value, exceeding 0.621, for GDP and electricity consumption, although it resulted in a lower R^2 value for population growth. Similar findings by Shi et al. (2023) confirmed the inverse relationship between urban entity growth and population density. The R^2 value for their correlation results between urban entity and population density was higher than 0.564. Liu S. et al. (2022) discovered that suburban development is closely associated with factors such as GDP, road network expansion, and population growth. Especially, Liu S. et al. (2022) found a higher consistency in suburban development with population density and road network expansion within the Pearl River Delta (PRD) agglomeration during the period from 2012 to 2020. The R^2 value of their correlation analysis was also higher than 0.500 for three variables: GDP, population density, and road network.

4.3 Limitations and Future Research Directions

At a larger spatial scale, errors in NPP-VIIRS data may arise due to atmospheric turbidity, distortion, and variations in satellite views (Ma Q. et al., 2014; Li & Li, 2015). Indeed, these factors can also have adverse effects on the accuracy of urban extraction results of our study. Also, in future research, it is essential to address the challenges associated with light emissions across different wavelengths. Moreover, the time bias in NPP-VIIRS data acquisition can have a detrimental impact on urban extraction results, particularly considering that a significant portion of artificial lights in Chinese cities are turned off after late nights (Ma Q. et al., 2014). Therefore, conducting a comparative study that utilizes LuoJia1-01 data for future research may offer advantages, as it has the potential to compensate for the limitations present in NPP-VIIRS data.

Although NTL data is valuable for evaluating urbanization, it's essential to recognize that the brightness of lights varies among cities based on their respective levels of urbanization, industrial structure, and development status (Ma Q. et al., 2014; Pan & Li, 2016). Hence, our study's findings may be adversely influenced to some extent by these factors. Certain cities in China utilize artificial lighting to attract tourists and improve the aesthetic appeal of their nighttime skyline. This can impact or elevate the brightness levels recorded for these cities (Cao, 2008; Ma Q. et al., 2014). Therefore, further research is needed to differentiate the unit values of NTL based on varying socioeconomic status. Additionally, previous research has demonstrated that NTL in industrial areas can influence and supplant peak pixel values within cities (Li & Li, 2015). Hence, adopting advanced image processing techniques to mitigate the influence of concentrated industrial plants within cities and the edges of cities on light brightness differentiation could potentially yield more reliable results, as also suggested by Ma Q. et al. (2014). Furthermore, while nighttime light data provides insight into human activity at the city scale, it may not fully account for peak pixel variations at the agglomeration scale. Therefore, in future research, it is essential to give due consideration to minimizing the impact of this limitation.

5. CONCLUSION

Using SNPP-VIIRS-like data (2000-2020) and NPP-VIIRS (2012-2020), we applied a novel k-means technique to extract urban and suburban entities in China. The research findings indicate a substantial expansion of urban entities at the prefecture level, increasing from 16,209 km² to 89,631 km² during the specified period. However, the total areas of urban entity features in our study differ from the findings of Shi et al. (2023), who reported urban areas ranging from 9,435 km² to 78,546 km². This discrepancy may be attributed to variations in the minimum distance decision rule employed in the k-means classification. The highest growth in urban entities was reported in the east and south prefectures, totaling 27,640 km² and 9,340 km², respectively. Conversely, the lowest growth was reported in the northeast (2,897 km²) and northwest (5,207 km²) prefectures. Yangtze River Delta exhibited the highest urbanization rate, experiencing a significant expansion of built-up areas from 2,684 km² to 41,465 km². The urban entities in all prefecture cities in the eastern provinces have significantly expanded, including provincial capitals like Shanghai, Hangzhou, Fuzhou, Jinan, Nanchang, Nanjing, and Hefei. As a key urban center in the Eastern region, Shanghai has experienced significant growth, expanding from 660 km² to 2852 km², demonstrating a growth rate of 45%. Further analysis revealed that the overall area of suburbs expanded from 59,151 km² to 120,339 km² between 2012 and 2020, indicating a proportional growth rate ranging from 0.4% to 1.9%. These results closely resemble the findings of Liu S. et al. (2022), who also used k-means classification algorithm for suburbs extraction and observed fluctuating trends in China, reporting growth rates ranging from 0.6% to 1.6% over nine years. Guizhou, Hunan, and Hubei provinces have exhibited suburban growth rates of 334%, 258%, and 246% respectively while Beijing, Guangdong, Tianjin, and Shanghai have experienced relatively low growth rates of 50%, 56%, 46%, and 17%. These findings are considered reliable, given that the OA and Kappa values of the outputs were within acceptable ranges, ranging from 77.2% to 92.3% for OA and from 0.77 to 0.88 for Kappa. Additionally, our study revealed a strong correlation between urban growth, urban GDP, and electricity consumption on a provincial scale. However, the limitations identified in our study must be carefully considered in future research focused on obtaining accurate urban extraction results. Indeed, incorporating alternative methods that are superior to the k-means algorithm or conducting comparative studies with other techniques would be highly beneficial in addressing these challenges and advancing the reliability of urban extraction from NTL remote sensing data in the future.

AUTHOR CONTRIBUTIONS

Conceptualization, N.C. and J.S.; methodology, N.C.; title, N.C.; formal analysis, N.C.; data curation, N.C.; manuscript-original draft, N.C.; manuscript-review and editing, J.S.; visualization, N.C.; supervision, J.S. All authors have read and legally accepted the final version of the article published in the journal.

ACKNOWLEDGEMENT

The authors express their gratitude to the Earth Observation Group and Oak Ridge National Laboratory for providing freely available SNPP-VIIRS data.

CONFLICT OF INTEREST

The authors declare no conflict of interest.

REFERENCES

- Cao, X. (2008). Research on the countermeasures for developing night tourism in Chinese cities. *Exploration of Economic Issues*, 8, 125-128. (in Chinese) <https://doi.org/10.3969/j.issn.1006-2912.2008.08.025>
- Chen, Z., Yu, B., Yang, C., Zhou, Y., Yao, S., Qian, X., Wang, C., Wu, B., & Wu, J. (2021). An extended time series (2000–2018) of global NPP-VIIRS-like nighttime light data from a cross-sensor calibration. *Earth System Science Data*, 13(3), 889-906. <https://doi.org/10.5194/essd-13-889-2021>
- Chen, Z., Yu, B., Yang, C., Zhou, Y., Yao, S., Qian, X., Wang, C., Wu, B., & Wu, J. (2020). An extended time-series (2000-2023) of global NPP-VIIRS-like nighttime light data [dataset]. Harvard Dataverse. <https://doi.org/10.7910/DVN/YGIVCD>

- Dai, J., Dong, J., Yang, S., & Sun, Y., (2021). Identification method of urban fringe area based on spatial mutation characteristics. *Journal of Geo-Information Science*, 23(8), 1401–1421. <https://doi.org/10.12082/dqxkx.2021.200502>
- Delmelle, E. C. (2015). Five decades of neighborhood classifications and their transitions: A comparison of four US cities, 1970–2010. *Applied Geography*, 57, 1–11. <https://doi.org/10.1016/j.apgeog.2014.12.002>
- Elvidge, C. D., Sutton, P. C., Ghosh, T., Tuttle, B. T., Baugh, K. E., Bhaduri, B., & Bright, E. (2009). A Global Poverty Map Derived from Satellite Data. *Computers & Geosciences*, 35(8), 1652–1660. <https://doi.org/10.1016/j.cageo.2009.01.009>
- Ellison, G., Glaeser, E. L., & Kerr, W. R. (2010). What causes industry agglomeration? Evidence from coagglomeration patterns. *American Economic Review*, 100(3), 1195–1213. <https://doi.org/10.1257/aer.100.3.1195>
- Fan, J., Ma, T., Zhou, C., Zhou, Y., & Xu, T. (2014). Comparative estimation of urban development in China's cities using socioeconomic and DMSP/OLS night light data. *Remote Sensing*, 6(8), 7840–7856. <https://doi.org/10.3390/rs6087840>
- Feng, Z., Peng, J., & Wu, J. (2020). Using DMSP/OLS nighttime light data and K-means method to identify urban–rural fringe of megacities. *Habitat International*, 103, 102227. <https://doi.org/10.1016/j.habitatint.2020.102227>
- Grove, J. M., Cadenasso, M. L., Pickett, S. T. A., Machlis, G. E., & Burch Jr. W. R. (2015). *The Baltimore School of Urban Ecology*. Yale University Press.
- Habitat, UN., Arctic Public Academy of Sciences, & FGUP “Russian State Scientific Research and Design Institute of Urbanistics”. (2006, April 26–27). ANNOTATION of the concept of the United Nations Human Settlements Programme (UN-HABITAT) project: “Sustainable Development of Cities in Arctic Region through the Improvement of their Engineering and Transportation Infrastructure and Personnel Training for Good Urban Governance”. In: 3rd SAO Meeting, Syktyvkar, Russia. <https://hdl.handle.net/11374/681>
- He, Z., Xu, S., Shen, W., Long, R., & Chen, H. (2017). Impact of urbanization on energy-related CO₂ emission at different development levels: regional difference in China based on panel estimation. *Journal of Cleaner Production*, 140(Part 3), 1719–1730. <https://doi.org/10.1016/j.jclepro.2016.08.155>
- Hu, X., Qian, Y., Pickett, S. T. A., & Zhou, W. (2020). Urban mapping needs up-to-date approaches to provide diverse perspectives of current urbanization: A novel attempt to map urban areas with nighttime light data. *Landscape Urban Planning*, 195, 103709. <https://doi.org/10.1016/j.landurbplan.2019.103709>
- Huang, Y., Wu, C., Chen, M., Yang, J., & Ren, H., (2020). A Quantile Approach for Retrieving the “Core Urban-Suburban-Rural” (USR) Structure Based on Nighttime Light. *Remote Sensing*, 12(24), 4179. <https://doi.org/10.3390/rs12244179>
- Imhoff, M. L., Lawrence, W. T., Stutzer, D. C., & Elvidge, C. D. (1997). A technique for using composite DMSP/OLS “City Lights” satellite data to map urban area. *Remote Sensing of Environment*, 61(3), 361–370. [https://doi.org/10.1016/S0034-4257\(97\)00046-1](https://doi.org/10.1016/S0034-4257(97)00046-1)
- Jia, W., Zhao, S., Zhang, X., Liu, S., Henebry, G. M., & Liu, L. (2021). Urbanization imprint on land surface phenology: The urban-rural gradient analysis for Chinese cities. *Global Change Biology*, 27(12), 2895–2904. <https://doi.org/10.1111/gcb.15602>
- Li, D., & Li, X. (2015). An overview on data mining of nighttime light remote sensing. *Acta Geodesy and Cartography Sinica*, 44(6), 591–601.
- Li, X., Gong, P., & Liang, L.A. (2015). A 30-year (1984–2013) record of annual urban dynamics of Beijing City derived from Landsat data. *Remote Sensing of the Environment*, 166, 78–90. <https://doi.org/10.1016/j.rse.2015.06.007>
- Lin, Z., Xu, H., & Huang, S. (2019). Monitoring of the Urban Expansion Dynamics in China's East Coast Using DMSP/OLS Nighttime Light Imagery. *Journal of Geographical Information Science*, 21(7), 1074–1085.

- Liu, S., Shi, K., & Wu, Y. (2022). Identifying and evaluating suburbs in China from 2012 to 2020 based on SNPP–VIIRS nighttime light remotely sensed data. *International Journal of Applied Earth Observation and Geoinformation*, 114, 103041. <https://doi.org/10.1016/j.jag.2022.103041>
- Liu, Z., He, C., Zhang, Q., Huang, Q., & Yang, Y. (2012). Extracting the dynamics of urban expansion in China using DMSP-OLS nighttime light data from 1992 to 2008. *Landscape and Urban Planning*, 106(1), 62-72. <https://doi.org/10.1016/j.landurbplan.2012.02.013>
- Lu, L., Zhang, Y., & Luo, T. T. (2014). Difficulties and Strategies in the Process of Population Urbanization: A Case Study in Chongqing of China. *Open Journal of Social Sciences*, 2(12), 90-95. <https://doi.org/10.4236/jss.2014.212013>
- Luo, T., Zeng, J., Chen, W., Wang, Y., Gu, T., & Huang, C. (2023). Ecosystem services balance and its influencing factors detection in China: A case study in Chengdu-Chongqing urban agglomerations. *Ecological Indicators*, 151, 110330. <https://doi.org/10.1016/j.ecolind.2023.110330>
- Ma, M., Lang, Q., Yang, H., Shi, K., & Ge, W. (2020). Identification of Polycentric Cities in China Based on NPP-VIIRS Nighttime Light Data. *Remote Sensing*, 12(19), 3248. <https://doi.org/10.3390/rs12193248>
- Ma, Q., He, C., Wu, J., Liu, Z., Zhang, Q., & Sun, Z. (2014). Quantifying spatiotemporal patterns of urban impervious surfaces in China: An improved assessment using nighttime light data. *Landscape Urban Planning*, 130, 36-49. <https://doi.org/10.1016/j.landurbplan.2014.06.009>
- Ma, T., Zhou, C., Pei, T., Haynie, S., & Fan, J. (2012). Quantitative estimation of urbanization dynamics using time series of DMSP/OLS nighttime light data: A comparative case study from China's cities. *Remote Sensing of Environment*, 124, 99-107. <https://doi.org/10.1016/j.rse.2012.04.018>
- Ma, T., Zhou, Y., Zhou, C., Haynie, S., Pei, T., & Xu, T. (2015). Night-time light derived estimation of spatiotemporal characteristics of urbanization dynamics using DMSP/OLS satellite data. *Remote Sensing of Environment*, 158, 453-464. <https://doi.org/10.1016/j.rse.2014.11.022>
- National Bureau of Statistics. (2000-2020). *City Statistical Yearbook*. China Statistics Press: Beijing, China (Accessed:17/09/2023). <https://data.cnki.net/yearBook/single?id=N2022040095>
- Pan, J., & Li, J. (2016). Estimate and Spatio-Temporal Dynamics of Electricity Consumption in China Based on DMSP/OLS Images. *Geographical Research*, 35(4), 627-638.
- Schneider, A., Friedl, M. A., & Potere, D. (2010). Mapping global urban areas using MODIS 500-m data: New methods and datasets based on urban ecoregions. *Remote Sensing of Environment*, 114(8), 1733-1746. <https://doi.org/10.1016/j.rse.2010.03.003>
- Shi, K., Chen, Y., Yu, B., Xu, T., Li, L., Huang, C., Liu, R., Chen, Z., & Wu, J. (2016). Urban Expansion and Agricultural Land Loss in China: A Multi-scale Perspective. *Sustainability*, 8(8), 790. <https://doi.org/10.3390/su8080790>
- Shi, K., Wu, Y., Liu, S., Chen, Z., Huang, C., & Cui, Y. (2023). Mapping and evaluating global urban entities (2000–2020): A novel perspective to delineate urban entities based on consistent nighttime light data. *GIScience & Remote Sensing*, 60(1), 2161199. <https://doi.org/10.1080/15481603.2022.2161199>
- Su, Y., Chen, X., Wang, C., Zhang, H., Liao, J., Ye, Y., & Wang, C. (2015). A new method for extracting built-up urban areas using DMSP-OLS nighttime stable lights: A case study in the Pearl River Delta, southern China. *GIScience & Remote Sensing*, 52(2), 218-238. <https://doi.org/10.1080/15481603.2015.1007778>
- Sun, Y., & Zhao, S. (2018). Spatiotemporal dynamics of urban expansion in 13 cities across the Jing-Jin-Ji urban agglomeration from 1978 to 2015. *Ecological Indicators*, 87, 302-313. <https://doi.org/10.1016/j.ecolind.2017.12.038>
- Thapa, R. B., & Murayama, Y. (2009). Examining Spatiotemporal Urbanization Patterns in Kathmandu Valley, Nepal: Remote Sensing and Spatial Metrics Approaches. *Remote Sensing*, 1(3), 534-556. <https://doi.org/10.3390/rs1030534>

- Tian, Y. (2020). Mapping suburbs based on spatial interactions and effect analysis on ecological landscape change: A case study of Jiangsu province from 1998 to 2018, eastern China. *Land*, 9(5), 159. <https://doi.org/10.3390/land9050159>
- Tian Y., & Qian, J. (2021). Suburban identification based on multi-source data and landscape analysis of its construction land: A case study of Jiangsu Province, China. *Habitat International*, 118, 102459. <https://doi.org/10.1016/j.habitatint.2021.102459>
- United Nations, Department of Economic and Social Affairs, Population Division (2019). World Urbanization Prospects: The 2018 Revision (ST/ESA/SER.A/420). New York: United Nations. <https://population.un.org/wup/publications/Files/WUP2018-Report.pdf>
- Wijesinghe, W. M. D. C., & Withanage, W. K. N. C. (2021). Detection of the changes in land use and land cover using remote sensing and GIS in Thalawa DS Division. *Prathimana Journal*, 14(1), 72–86
- Withanage, W. K. N. C., Mishra, P. K., & Jayasinghe, B. C. (2024). An Assessment of Spatio-temporal Land Use/Land Cover Dynamics Using Landsat Time Series Data (2008-2022) in Kuliypitiya West Divisional Secretariat Division in Kurunagala District, Sri Lanka. *Journal of Geospatial Surveying*, 4(1), 12-23. <https://doi.org/10.4038/jgs.v4i1.52>
- Withanage, N. C., Shi, K., & Shen, J. (2023). Extracting and Evaluating Urban Entities in China from 2000 to 2020 Based on SNPP-VIIRS-like Data. *Remote Sensing*, 15(18), 4632. <https://doi.org/10.3390/rs15184632>
- Xiao, P., Wang, X., Feng, X., Zhang, X., & Yang, Y. (2014). Detecting China's Urban Expansion over the Past Three Decades Using Nighttime Light Data. *IEEE Journal of Selected Topics in Applied Earth Observations and Remote Sensing*, 7(10), 4095-4106. <https://doi.org/10.1109/JSTARS.2014.2302855>
- Xu, T., Ma, T., Zhou, C., & Zhou, Y. (2014). Characterizing Spatio-Temporal Dynamics of Urbanization in China Using Time Series of DMSP/OLS Night Light Data. *Remote Sensing*, 6(8), 7708-7731. <https://doi.org/10.3390/rs6087708>
- Yang, Y., Ma, M., Tan, C., & Li, W. (2017). Spatial Recognition of the Urban-Rural Fringe of Beijing Using DMSP/OLS Nighttime Light Data. *Remote Sensing*, 9(11), 1141. <https://doi.org/10.3390/rs9111141>
- Yu, B., Tang, M., Wu, Q., Yang, C., Deng, S., Shi, K., Peng, C., Wu, J., & Chen, Z. (2018). Urban Built-Up Area Extraction From Log-Transformed NPP-VIIRS Nighttime Light Composite Data. *IEEE Geoscience and Remote Sensing Letters*, 15(8), 1279-1283. <https://doi.org/10.1109/LGRS.2018.2830797>
- Yuh, Y. G., Tracz, W., Matthews, H. D., Turner, S. E. (2023). Application of machine learning approaches for land cover monitoring in northern Cameroon. *Ecological Informatics*, 74, 101955. <https://doi.org/10.1016/j.ecoinf.2022.101955>
- Zhang, Q., & Seto, K. C. (2011). Mapping urbanization dynamics at regional and global scales using multi-temporal DMSP/OLS nighttime light data. *Remote Sensing of Environment*, 115(9), 2320-2329. <https://doi.org/10.1016/j.rse.2011.04.032>
- Zhang, H., Liang, C., & Pan, Y. (2022). Spatial Expansion of Built-Up Areas in the Beijing-Tianjin-Hebei Urban Agglomeration Based on Nighttime Light Data: 1992-2020. *International Journal of Environmental Research and Public Health*, 19(7), 3760. <https://doi.org/10.3390/ijerph19073760>
- Zhang, X., Liu, L., Wu, C., Chen, X., Gao, Y., Xie, S., & Zhang, B. (2020). Development of a global 30 m impervious surface map using multi-source and multi-temporal remote sensing datasets with the Google Earth Engine platform. *Earth System Science Data*, 12(3), 1625-1648. <https://doi.org/10.5194/essd-12-1625-2020>
- Zheng, Y., Tang, L., & Wang, H. (2021). An improved approach for monitoring urban built-up areas by combining NPP-VIIRS nighttime light, NDVI, NDWI, and NDBI. *Journal of Cleaner Production*, 328, 129488. <https://doi.org/10.1016/j.jclepro.2021.129488>
- Zhou, Q., Li, B., & Sun, B. (2008, July 3-11). *Modelling spatio-temporal pattern of landuse change using multi-temporal remotely sensed imagery*. In: Proceedings of the 21st Congress of the International Society for Photogrammetry and Remote Sensing, ISPRS 2008, (Vol. 37, Part B7), (pp. 729-734), Beijing, China.

Zhou, Y., Smith, S. J., Elvidge, C. D., Zhao, K., Thomson, A., & Imhoff, M. (2014). A cluster-based method to map urban area from DMSP/OLS nightlights. *Remote Sensing of Environment*, 147, 173-185. <https://doi.org/10.1016/j.rse.2014.03.004>